

# Insulator-to-metal phase transition in Yb-based Kondo insulators

Guang-Bin Li and Guang-Ming Zhang

*Department of Physics, Tsinghua University, Beijing 100084, China*

Lu Yu

*Institute of Physics, Chinese Academy of Sciences, Beijing 100190, China;*

*Institute of Theoretical Physics, Chinese Academy of Sciences, Beijing 100190, China*

(Dated: April 18, 2022)

The periodic Anderson lattice model for the crystalline electric field (CEF) split 4f quartet states is used to describe the Yb-based Kondo insulators/semiconductors. In the slave-boson mean-field approximation, we derive the hybridized quasiparticle bands, and find that decreasing the hybridization difference of the two CEF quartets may induce an insulator-to-metal phase transition. The resulting metallic phase has a hole and an electron Fermi pockets. Such a phase transition may be realized experimentally by applying pressure, reducing the difference in hybridization of the two CEF quartets.

PACS numbers: 71.27.+a, 75.30.Mb, 75.20.Hr

Kondo insulators or semiconductors, such as YbB<sub>12</sub>, belong to strongly correlated electron systems<sup>1,2</sup>, in which the conduction electrons hybridize with the localized 4f-electrons and the strong Coulomb repulsion results in highly renormalized quasiparticle bands with a small indirect energy gap<sup>3-6</sup>. To study the characteristic properties of these materials at low temperatures, some experiments have been attempted to make the insulating gap vanish by applying an external magnetic field<sup>7,8</sup> or pressure<sup>9</sup>, leading to an insulator-metal phase transition. Such a transition under the external magnetic field has been considered in the previous studies<sup>10-13</sup>, however, the microscopic mechanism for the pressure induced insulator-to-metal transition remains far from being fully understood.

For the Yb-based Kondo insulators, an external pressure can affect the hybridization between 5d band electrons and the more atomic-like 4f electrons, giving rise to the intermediate valence behavior. The Yb valence is directly related to the number of 4f-holes  $n_h$  by  $v = 2 + n_h$ . At the ambient pressure,  $n_h$  spans a broad range between 0 and 1 in Yb-based compounds, and the intermediate valence reflects the hybridization of the energetically close Yb<sup>2+</sup> (4f<sup>14</sup>) and Yb<sup>3+</sup> (4f<sup>13</sup>) configurations. The electronic configuration of Yb<sup>3+</sup> (4f<sup>13</sup>) can be regarded as a single hole in the 4f-shell, while the configuration of Yb<sup>2+</sup> (4f<sup>14</sup>) corresponds to the closed 4f-shell. Taking into account the much larger strength (1.3eV) of the spin-orbit coupling<sup>14</sup>, a  $j = 7/2$  f-hole state is split into a quartet and two doublet states by the crystalline electric field (CEF) under the cubic symmetry, which is the usual lattice structure of YbB<sub>12</sub>. These two doublets are almost degenerate and may be treated as a quasi-quartet. Thus, a periodic Anderson lattice model with  $U \rightarrow \infty$  for the CEF split 4f states can be used to describe these Yb-based Kondo insulators or semiconductors<sup>15</sup>.

It has been further pointed out that the anisotropic hybridizations of the two CEF quartets play an important role in the formation of the two dispersive spin resonances

at the continuum threshold<sup>15</sup>, the most salient features observed by inelastic neutron scattering experiments in YbB<sub>12</sub> (Ref.5,6). Motivated by this analysis, we further notice that, above a threshold of the CEF splitting, decreasing the difference in the hybridization of the two CEF quartets may cause an overlap between the middle lower and upper hybridized quasiparticle bands, leading to an insulator-to-metal phase transition. Experimentally, this phase transition can be realized by applying pressure, reducing the difference in the hybridization of the two CEF quasi-quartets. Such a pressure induced insulator-to-metal transition has been observed in the Kondo insulator SmB<sub>6</sub>, where the electrical resistivity has been measured below 80 K and under pressure between 1 bar and 70 kbar (Ref.<sup>9</sup>). Above the critical pressure 40 kbar, a transition occurs from a Kondo insulator to a metallic heavy fermion liquid and a non-Fermi liquid behavior has been found<sup>9</sup>.

In this paper, we will carefully study the periodic Anderson model with  $U \rightarrow \infty$  for the CEF split 4f quartet states. Using the slave-boson mean-field approximation, we will derive four quasiparticle bands resulting from the hybridization between the conduction electrons and localized 4f-hole states, and find that decreasing the hybridization difference of the two CEF quartets indeed induce an insulator-to-metal phase transition. The resulting metallic phase has a hole and an electron Fermi pockets. By including the Coulomb interaction between the localized and conduction electrons, we discuss the possible instability of the resulting metallic phase.

To describe the Yb-based Kondo insulators or semiconductors, the periodic Anderson lattice model with  $U \rightarrow \infty$  for the CEF split 4f states has been introduced<sup>15</sup>

$$\mathcal{H} = \sum_{\mathbf{k}, \gamma} \epsilon_{\mathbf{k}} d_{\mathbf{k}\gamma}^{\dagger} d_{\mathbf{k}\gamma} + \sum_{\mathbf{k}, \gamma} (\epsilon_f + \Delta_{\gamma}) f_{i\gamma}^{\dagger} f_{i\gamma} + \frac{1}{\sqrt{\mathcal{N}}} \sum_{i, \mathbf{k}, \gamma} (V_{\mathbf{k}\gamma} e^{i\mathbf{k} \cdot \mathbf{R}_i} f_{i, \gamma}^{\dagger} d_{\mathbf{k}\gamma} b_i + h.c.), \quad (1)$$

where the first term denotes the conduction electron band, the second term stands for the binding energy of the 4f-hole, and  $\Delta_\gamma$  ( $\Delta_1 = 0, \Delta_2 = \Delta$ ) is the CEF splitting energy for the two quasi-quartets with  $\gamma = (\Gamma, m)$ , where  $\Gamma = 1, 2$  denotes the quartets and  $m = 1 - 4$  represents the four-fold orbital degeneracy. Due to the exclusion of the double occupancy, a projection has been implemented by using the slave-boson representation<sup>16</sup>. Then the  $\text{Yb}^{2+}$  ( $4f^{14}$ ) configuration without a 4f-hole state can be accounted for by an auxiliary boson state  $b_i^\dagger |0\rangle$ , while the  $\text{Yb}^{3+}$  ( $4f^{13}$ ) configuration with a 4f-hole state is represented by a fermion state  $f_{i\gamma}^\dagger |0\rangle$ . The conduction electrons hybridize with the  $f$ -hole at each lattice site in both quartets with different strengths. At each lattice site the constraint  $Q_i = b_i^\dagger b_i + \sum_\gamma f_{i\gamma}^\dagger f_{i\gamma} = 1$  has to be enforced, and the total Hamiltonian is  $\mathcal{H} + \sum_i \lambda_i (Q_i - 1)$ , where  $\lambda_i$  is the Lagrange multiplier.

Now the slave-boson mean-field approximation is performed by neglecting the fluctuation of the Bose field  $\langle b_i^\dagger \rangle = \langle b_i \rangle = b$  and the site dependence of the local field  $\lambda_i = \lambda$ . Within these approximations, the mean-field model Hamiltonian can be written as

$$\mathcal{H}_{mf} = \sum_{\mathbf{k}, \gamma} [\epsilon_{\mathbf{k}} d_{\mathbf{k}\gamma}^\dagger d_{\mathbf{k}\gamma} + \tilde{\varepsilon}_\gamma f_{\mathbf{k}\gamma}^\dagger f_{\mathbf{k}\gamma} + \tilde{V}_\gamma (d_{\mathbf{k}\gamma}^\dagger f_{\mathbf{k}\gamma} + h.c.)] + \mathcal{N} \epsilon_0, \quad (2)$$

where  $\tilde{\varepsilon}_\gamma = \varepsilon_f + \Delta_\gamma + \lambda$  is the renormalized energy level of the localized states,  $\tilde{V}_\gamma = bV_\gamma$ , and  $\epsilon_0 = \lambda(b^2 - 1)$ . It should be noticed that the dependence of the hybridization strength on  $\mathbf{k}$  has been neglected, *i.e.*,  $V_{\mathbf{k}\gamma} = V_\gamma$ . Furthermore, we will replace  $V_\gamma$  by  $V_\Gamma$  for simplicity. By performing the Bogoliubov transformation

$$\alpha_{\mathbf{k}\gamma} = \mu_{\mathbf{k}\gamma} d_{\mathbf{k}\gamma} + \nu_{\mathbf{k}\gamma} f_{\mathbf{k}\gamma}, \quad \beta_{\mathbf{k}\gamma} = -\nu_{\mathbf{k}\gamma} d_{\mathbf{k}\gamma} + \mu_{\mathbf{k}\gamma} f_{\mathbf{k}\gamma}, \quad (3)$$

we can diagonalize the quadratic Hamiltonian and obtain

$$\mathcal{H}_{MF} = \sum_{\mathbf{k}, \gamma} \left( E_{\mathbf{k}\gamma}^+ \alpha_{\mathbf{k}\gamma}^\dagger \alpha_{\mathbf{k}\gamma} + E_{\mathbf{k}\gamma}^- \beta_{\mathbf{k}\gamma}^\dagger \beta_{\mathbf{k}\gamma} \right), \quad (4)$$

with four hybridized quasiparticle bands are

$$E_{\mathbf{k}\gamma}^\pm = \frac{1}{2} \left[ \epsilon_{\mathbf{k}} + \tilde{\varepsilon}_\gamma \pm \sqrt{(\epsilon_{\mathbf{k}} - \tilde{\varepsilon}_\gamma)^2 + 4\tilde{V}_\gamma^2} \right], \quad (5)$$

while the Bogoliubov parameters  $\mu_{\mathbf{k}\gamma}$  and  $\nu_{\mathbf{k}\gamma}$  are given by

$$\begin{pmatrix} \mu_{\mathbf{k}\gamma} \\ \nu_{\mathbf{k}\gamma} \end{pmatrix} = \frac{1}{\sqrt{2}} \left[ 1 \pm \frac{\epsilon_{\mathbf{k}} - \tilde{\varepsilon}_\gamma}{\sqrt{(\epsilon_{\mathbf{k}} - \tilde{\varepsilon}_\gamma)^2 + 4\tilde{V}_\gamma^2}} \right]^{1/2}. \quad (6)$$

These two parameters describe the contributions of the conduction electron band and localized  $f$ -hole band to the hybridized quasiparticles, respectively.

Moreover, the ground-state energy per site is given by

$$E_g = \frac{1}{\mathcal{N}} \sum_{\mathbf{k}, \gamma} \left[ E_{\mathbf{k}\gamma}^+ \theta(E_{\mathbf{k}\gamma}^+) + E_{\mathbf{k}\gamma}^- \theta(E_{\mathbf{k}\gamma}^-) \right] + \epsilon_0, \quad (7)$$

where  $\theta(E_{\mathbf{k}\gamma}^\pm)$  is the step function. The chemical potential  $\mu$  and the Lagrange multiplier  $\lambda$  have to be determined self-consistently according to the conservation of the total number of particle per lattice site  $n_c + n_f = 2$ . Depending on the parameter values  $\varepsilon_f$ ,  $\Delta$ , and  $V_\Gamma$ , the variational parameters  $b$  and  $\lambda$  are also determined self-consistently. From the hybridized quasiparticle band structure, the ground state of the system can be an insulating state, where the two lower bands are filled completely, leaving an indirect energy gap. As the  $\mathbf{k}$  dependence in  $E_g$  appears through the conduction electron energy  $\epsilon_{\mathbf{k}}$ , summations over  $\mathbf{k}$  can be transformed into an integral over energy  $\epsilon$  in the interval  $[-D, D]$ . By assuming a constant density of states, the ground-state energy is thus evaluated as

$$E_g = \frac{1}{8D} \sum_\Gamma \left\{ 4D\tilde{\varepsilon}_\Gamma - 4\tilde{V}_\Gamma^2 \ln \frac{\Lambda_\Gamma^-(D) + D - \tilde{\varepsilon}_\Gamma}{\Lambda_\Gamma^+(D) - D - \tilde{\varepsilon}_\Gamma} - [(D - \tilde{\varepsilon}_\Gamma)\Lambda_\Gamma^-(D) + (D + \tilde{\varepsilon}_\Gamma)\Lambda_\Gamma^+(D)] \right\} + \epsilon_0, \quad (8)$$

where  $\Lambda_\Gamma^\pm(x) = \sqrt{(x \pm \tilde{\varepsilon}_\Gamma)^2 + 4\tilde{V}_\Gamma^2}$ ,  $\tilde{\varepsilon}_2 = \tilde{\varepsilon}_1 + \Delta$ , and  $\tilde{V}_2 = bV_2 = b(V_1 + \delta V)$ . Minimizing the ground-state energy density with respect to  $b$  and  $\lambda$ , respectively, we obtain the following self-consistent equations

$$b^2 = \frac{1}{4D} \sum_\Gamma [\Lambda_\Gamma^+(D) - \Lambda_\Gamma^-(D)],$$

$$\lambda = \frac{1}{2D} \sum_\Gamma V_\Gamma^2 \ln \frac{\Lambda_\Gamma^-(D) + D - \tilde{\varepsilon}_\Gamma}{\Lambda_\Gamma^+(D) - D - \tilde{\varepsilon}_\Gamma}. \quad (9)$$

However, we notice that there exists another possible structure of the quasiparticle bands, where the chemical potential  $\mu$  cuts through the two middle hybridized quasiparticle bands  $E_{\mathbf{k}1}^+$  and  $E_{\mathbf{k}2}^-$  at  $\xi_1$  and  $\xi_2$ , respectively. Both these energy parameters are determined by the equation  $E_{\mathbf{k}1}^+ = E_{\mathbf{k}2}^- = \mu$ . From the condition of the total number of particles per lattice site  $n_c + n_f = 2$ , we can derive the result  $\xi_1 = -\xi_2 \equiv -\xi$  and

$$2\xi + \Delta = \Lambda_1^+(\xi) + \Lambda_2^-(\xi). \quad (10)$$

Here  $\xi$  can be used to characterize the insulator-to-metal transition. When  $0 < \xi < D$ , the ground state should be metallic, while for  $\xi = D$  the ground state corresponds to a critical point. The corresponding ground-state energy density in the metallic phase is thus expressed as

$$E_g = \frac{1}{4D} [(3D - \xi)\tilde{\varepsilon}_1 + (D + \xi)\tilde{\varepsilon}_2 + \xi^2 - D^2] + \frac{\tilde{V}_1^2}{2D} \ln \frac{\Lambda_1^+(\xi) - \xi - \tilde{\varepsilon}_1}{\Lambda_1^-(D) + D - \tilde{\varepsilon}_1} - \frac{\tilde{V}_2^2}{2D} \ln \frac{\Lambda_2^-(\xi) + \xi - \tilde{\varepsilon}_2}{\Lambda_2^+(D) - D - \tilde{\varepsilon}_2} - \frac{1}{8D} [(\xi + \tilde{\varepsilon}_1)\Lambda_1^+(\xi) + (D - \tilde{\varepsilon}_1)\Lambda_1^-(D)] - \frac{1}{8D} [(\xi - \tilde{\varepsilon}_2)\Lambda_2^-(\xi) + (D + \tilde{\varepsilon}_2)\Lambda_2^+(D)] + \epsilon_0. \quad (11)$$

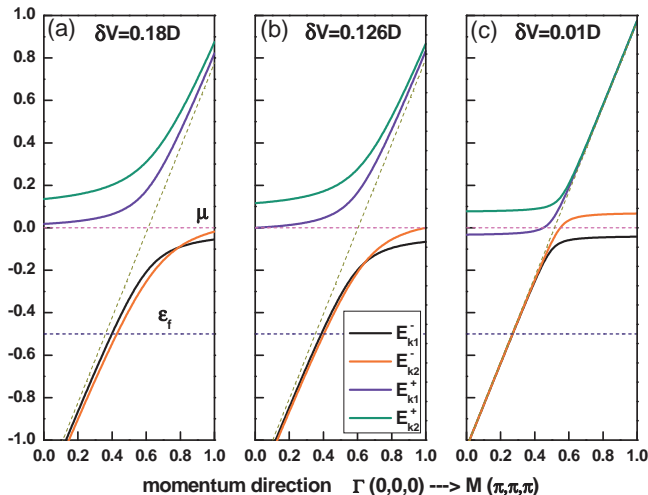


FIG. 1: (color online). The quasiparticle band structure for  $V_1 = 0.4D$ ,  $\epsilon_f = -0.5D$ , and  $\Delta = 0.1D$ . (a) Insulator phase, (b) Critical point, (c) Metallic phase.

By minimizing  $E_g$  with respect to  $b$  and  $\lambda$ , the corresponding self-consistent equations can be deduced to

$$b^2 = \frac{1}{4D} [\Lambda_1^+(\xi) - \Lambda_1^-(D) - \Lambda_2^-(\xi) + \Lambda_2^+(D)],$$

$$\lambda = \frac{V_1^2}{2D} \ln \frac{\Lambda_1^-(D) + D - \tilde{\epsilon}_1}{\Lambda_1^+(\xi) - \xi - \tilde{\epsilon}_1} + \frac{V_2^2}{2D} \ln \frac{\Lambda_2^-(\xi) + \xi - \tilde{\epsilon}_2}{\Lambda_2^+(D) - D - \tilde{\epsilon}_2}. \quad (12)$$

In order to deduce the ground state phase diagram, we should first numerically solve Eq.(9) for the insulating phase and Eqs.(10) and (12) for the metallic phase, respectively. The hybridized quasiparticle band energy versus the momentum along the diagonal direction  $\Gamma(0,0,0) \rightarrow M(\pi,\pi,\pi)$  are plotted in Fig.1 with  $V_1 = 0.4D$ ,  $\epsilon_f = -0.5D$ , and  $\Delta = 0.1D$  for three different values of  $\delta V$ . As shown in Fig.1(a) for  $\delta V = 0.18D$ , there opens an indirect gap between the middle upper and lower bands, corresponding to an insulating phase. In Fig.1(b) for  $\delta V = 0.126D$ , the middle upper and lower bands just meet at the chemical potential, corresponding the critical point of the transition. Since we have  $\xi = D$  at the critical point, the ground-state energies of the metallic and insulating phases are equal. So the insulator-metal transition is a continuous second-order phase transition. Finally, in Fig.1(c) for  $\delta V = 0.01D$ , the middle lower and upper bands overlap, and the chemical potential cuts through these two bands, which corresponds to the metallic phase.

The critical condition under which the insulator-metal transition occurs can be determined from Eq.(10) and Eq.(12) by setting  $\xi = D$ . Then the ground-state phase diagram can be constructed for  $V_1 = 0.4D$  and  $\epsilon_f = -0.5D$  and is shown in Fig.2(a). Clearly there exists a threshold of the CEF splitting energy  $\Delta_c$ , and only when  $\Delta > \Delta_c$  the insulator-to-metal phase transition occurs by turn-

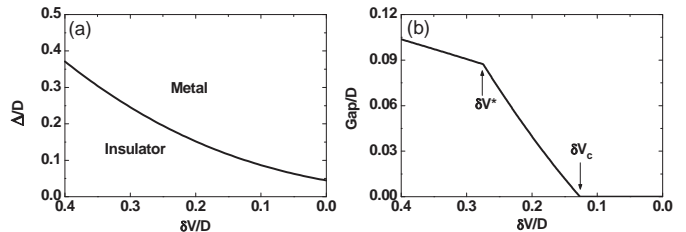


FIG. 2: (a) Ground state phase diagram for  $V_1 = 0.4D$  and  $\epsilon_f = -0.5D$ ; (b) Indirect energy gap as a function of the hybridization difference of the two CEF quartets  $\delta V$  for  $\Delta = 0.1D$ .

ing the difference in hybridization of the two CEF quasi-quartets. The change of the indirect gap is another evidence to characterize the insulator-to-metal phase transition, and can be also calculated and displayed in Fig.2(b) for  $\Delta = 0.1D$ . It shows that the indirect quasiparticle gap decreases almost linearly with decreasing the hybridization difference of the two CEF quartets, and this energy gap finally vanishes at  $\delta V_c$ . There is another critical value  $\delta V^*$ , where the top energy levels of the two lower quasiparticle bands interchange with each other around the Brillouin zone boundary. Then the indirect energy gap has a cusp.

Actually, such an insulator-to-metal phase transition can be realized experimentally. There exists a strong CEF splitting estimated in  $\text{YbB}_{12}$ , and we believe that increasing pressure can continuously reduce the difference in hybridization of the two CEF quasi-quartets. So below the critical value  $\delta V_c$ ,  $\text{YbB}_{12}$  is an insulator with an indirect gap as observed in experiments<sup>3-6</sup>, while above this critical value  $\delta V_c$  this material can transform into a heavy electron metal with an enhanced effective mass due to the presence of heavy charge carriers. Thus, our theory may provide a general microscopic mechanism of the pressure induced insulator-to-metal transition in Yb-based Kondo insulators/semiconductors.

Since a constant density of states for the conduction electron band was assumed in the above slave-boson mean-field calculation, the obtained results are independent of the dimensionality of the model. In order to see the special Fermi surface structure of the metallic phase, the model Hamiltonian Eq.(1) is redefined on a two-dimensional square lattice system with the conduction electron band

$$\epsilon_{\mathbf{k}} = -2t(\cos k_x + \cos k_y) + 4t' \cos k_x \cos k_y, \quad (13)$$

where  $t$  denotes the nearest neighbor hopping and  $t'$  denotes the next-nearest neighbor hopping. Then the same slave-boson mean field calculation can be performed, and the insulator-to-metal phase transition also takes place for a set of parameters  $V_1 = 0.4D$ ,  $\epsilon_f = -0.5D$ ,  $t = 0.25D$ , and  $t' = 0.3t$  when decreasing the parameter  $\delta V$ . In the metallic phase, we have calculated the corresponding Fermi surface structure shown in Fig.3. There

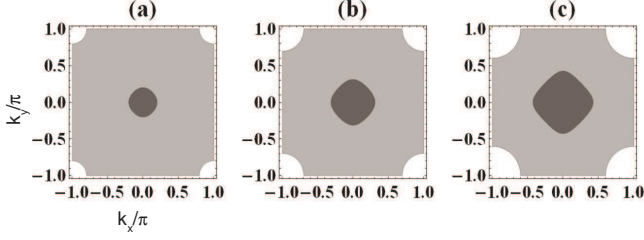


FIG. 3: (color online). Fermi surface structure of the two-dimensional model Hamiltonian on a square lattice with  $V_1 = 0.4D$ ,  $\Delta = 0.1D$ , and  $\epsilon_f = -0.5D$ . (a)  $\delta V = 0.08D$ , (b)  $\delta V = 0.05D$  and (c)  $\delta V = 0.01D$ .

exist two Fermi pockets: one electron-like in the center of the Brillouin zone and one hole-like in the corners of the Brillouin zone. These two Fermi pockets have exactly the same area in the Brillouin zone. Such a heavy electron metal corresponds to a semi-metal. Decreasing the hybridization difference  $\delta V$  below the critical value, the sizes of the electron and hole Fermi pockets become larger and larger, as displayed in Fig.3.

For the three dimensional Yb-based Kondo insulators/semiconductors, the Fermi surface of the resulting metallic phase should still be given by a hole and an electron pockets. As the temperature is lowered enough, some instabilities may further appear. Due to the presence of the strong mixed valence effect in such systems, the additional on-site Coulomb interaction between the conduction electrons and localized  $f$ -hole should be taken into account. In the slave-boson representation, it is given by

$$\mathcal{H}_I = U_{fc} \sum_i \sum_{\gamma\gamma'} f_{i\gamma}^\dagger f_{i\gamma} d_{i\gamma'}^\dagger d_{i\gamma'}. \quad (14)$$

When the coupling strength  $U_{fc}$  is assumed to be small, we can rewrite this additional interaction in terms of the hybridized quasiparticles as

$$\begin{aligned} \mathcal{H}_I = \frac{U_{fc}}{\mathcal{N}} \sum_{\mathbf{k}_1 \mathbf{k}_2 \mathbf{k}_3 \mathbf{k}_4} & \left( \nu_{\mathbf{k}_1 1} \mu_{\mathbf{k}_2 1} \nu_{\mathbf{k}_3 1} \mu_{\mathbf{k}_4 1} \alpha_{\mathbf{k}_3 1}^\dagger \alpha_{\mathbf{k}_1 1} \alpha_{\mathbf{k}_4 1}^\dagger \alpha_{\mathbf{k}_2 1} \right. \\ & + \mu_{\mathbf{k}_1 2} \nu_{\mathbf{k}_2 2} \mu_{\mathbf{k}_3 2} \nu_{\mathbf{k}_4 2} \beta_{\mathbf{k}_3 2}^\dagger \beta_{\mathbf{k}_1 2} \beta_{\mathbf{k}_4 2}^\dagger \beta_{\mathbf{k}_2 2} \\ & + \nu_{\mathbf{k}_1 1} \nu_{\mathbf{k}_2 2} \nu_{\mathbf{k}_3 1} \nu_{\mathbf{k}_4 2} \alpha_{\mathbf{k}_3 1}^\dagger \alpha_{\mathbf{k}_1 1} \beta_{\mathbf{k}_4 2}^\dagger \beta_{\mathbf{k}_2 2} \\ & \left. + \mu_{\mathbf{k}_1 2} \mu_{\mathbf{k}_2 1} \mu_{\mathbf{k}_3 2} \mu_{\mathbf{k}_4 1} \beta_{\mathbf{k}_3 2}^\dagger \beta_{\mathbf{k}_1 2} \alpha_{\mathbf{k}_4 1}^\dagger \alpha_{\mathbf{k}_2 1} \right), \quad (15) \end{aligned}$$

where  $\mathbf{k}_1 + \mathbf{k}_2 = \mathbf{k}_3 + \mathbf{k}_4$  should be satisfied and *only* the two quasiparticle bands, crossing the Fermi energy, have been taken into account.  $\alpha_{\mathbf{k},1}$  and  $\alpha_{\mathbf{k},1}^\dagger$  are defined on the

electron Fermi pocket, while  $\beta_{\mathbf{k},2}$  and  $\alpha_{\mathbf{k},2}^\dagger$  are defined on the hole Fermi pocket. Among these residual quasiparticle interactions, the first two terms represent the intra-pocket scatterings with a small momentum transfer, while the last two terms correspond to the inter-pocket scatterings with a large momentum transfer.

According to the recent renormalization group analysis for a two-band interacting model with electron and hole Fermi pockets<sup>17</sup>, the inter-pocket quasiparticle interactions will determine the possible instabilities at low temperatures. When we set  $\mathbf{q}$  as a small momentum and  $\mathbf{Q}$  as a large momentum which is the distance between the centers of two Fermi pockets, then inter-pocket quasiparticle interactions can be approximated as

$$\begin{aligned} -\frac{U_{fc}}{\mathcal{N}} \sum_{\mathbf{q}\mathbf{q}'} & (\mu_{\mathbf{q}1} \mu_{\mathbf{q}'1} \mu_{\mathbf{q}2} \mu_{\mathbf{q}'2} + \nu_{\mathbf{q}1} \nu_{\mathbf{q}'1} \nu_{\mathbf{q}2} \nu_{\mathbf{q}'2}) \\ & \times \alpha_{\mathbf{q},1}^\dagger \beta_{\mathbf{Q}+\mathbf{q},2} \beta_{\mathbf{Q}+\mathbf{q}',2}^\dagger \alpha_{\mathbf{q}',1}. \quad (16) \end{aligned}$$

If there is a strong nesting between the hole and electron Fermi pockets, this inter-pocket repulsive interaction will further induce a particle-hole pairing instability, corresponding to an orbital-density wave ordering. The corresponding order parameter is given by  $\langle \alpha_{\mathbf{q}1}^\dagger \beta_{\mathbf{Q}+\mathbf{q}2} \rangle$  or  $\langle \beta_{\mathbf{Q}+\mathbf{q}'2}^\dagger \alpha_{\mathbf{q}'1} \rangle$ . Such a new type of ordering in heavy fermion materials will be discussed in our further investigations.

In conclusion, we have studied the Yb-based Kondo insulators with a strong CEF splitting in the framework of the periodic Anderson lattice model by using the slave-boson mean-field approximation. The obtained ground-state phase diagram and the indirect gap have demonstrated that a second-order insulator-to-metal transition occurs via reducing the hybridization difference of the two CEF quasi-quartets. Our theory provides a general microscopic mechanism of the pressure induced insulator-to-metal transition, because increasing the external pressure can effectively reduce the anisotropy of the hybridization strengths of the two CEF quartets experimentally. The resulting metallic phase has a hole and an electron Fermi pockets, which may exhibit an instability of an orbital-density wave ordering at low temperatures when the inter-pocket quasiparticle residual interactions are taken into account. These theoretical results are certainly needed to be confirmed experimentally in the future.

The authors would like to thank Dung-Hai Lee for his stimulating discussions and Yu Liu for his helps in the numerical calculations. This work is partially supported by NSF-China and the National Program for Basic Research of MOST, China.

<sup>1</sup> G. Aeppli and Z. Fisk, Comments Cond. Mat. Phys. **16**, 155-165 (1992).

<sup>2</sup> P. S. Riseborough, Adv. Phys. **49**, 257 (2000).

<sup>3</sup> T. Susaki, *et. al.*, Phys. Rev. Lett. **77**, 4269 (1996).

- <sup>4</sup> H. Okamura, S. Kimura, H. Shinozaki, T. Nanba, F. Iga, N. Shimizu, and T. Takabatake, *Phys. Rev. B* **58**, 7496 (1998).
- <sup>5</sup> J. M. Mignot, P. A. Alekseev, K. S. Nemkovski, L. P. Regnault, F. Iga, and T. Takabatake, *Phys. Rev. Lett.* **94**, 247204 (2005).
- <sup>6</sup> K. S. Nemkovski, *et al.*, *Phys. Rev. Lett.* **99**, 137204 (2007).
- <sup>7</sup> K. Sugiyama, F. Iga, M. Kasaya, T. Kasuya, and M. Date, *J. Phys. Soc. Jpn.* **57**, 3946 (1988).
- <sup>8</sup> M. Jaime, R. Movshovich, G. R. Stewart, W. P. Beyersmann, M. G. Berisso, M. F. Hundley, P. C. Canfield, and J. L. Sarrao, *Nature* **405**, 160 (2000).
- <sup>9</sup> S. Gabáni, E. Bauer, S. Berger, K. Flachbart, Y. Paderno, C. Paul, V. Pavlík, and N. Shitsevalova, *Phys. Rev. B* **67**, 172406 (2003).
- <sup>10</sup> K. S. D. Beach, P. A. Lee, and P. Monthoux, *Phys. Rev. Lett.* **92**, 026401 (2004).
- <sup>11</sup> I. Milat, F. Assaad, and M. Sgrist, *Eur. Phys. J. B* **38**, 571 (2004).
- <sup>12</sup> T. Ohashi, A. Koga, S. Suga, and N. Kawakami, *Phys. Rev. B* **70**, 245104 (2004).
- <sup>13</sup> T. Izumi, Y. Imai, and T. Saso, *J. Phys. Soc. Jpn.* **76**, 4715 (2007).
- <sup>14</sup> N. Martensson, B. Reihl, R. A. Pollak, F. Holtzheng, G. Kaindl, *Phys. Rev. B* **25**, 6522 (1982).
- <sup>15</sup> A. Akbari, P. Thalmeier and P. Fulde, *Phys. Rev. Lett.* **102**, 106402 (2009).
- <sup>16</sup> P. Coleman, *Phys. Rev. B* **29**, 3035 (1984).
- <sup>17</sup> A. V. Chubukov, D. Efremov, and I. Eremin, *Phys. Rev. B* **78**, 134512 (2008).